An Integrin-Independent Kaposi's Sarcoma-Associated Herpesvirus Infection Mechanism

Allison Alwan TerBush,[a] Florianne Hafkamp,[b] Ella Hartenian,[a] Hee Jun Lee,[a] Britt A Glaunsinger,[a,c,d] Laurent Coscoy[a]#

[a]Department of Molecular and Cell Biology, University of California, Berkeley, California, USA

[b]Graduate School of Life Sciences, Utrecht University, Utrecht, Netherlands

[c]Howard Hughes Medical Institute, University of California, Berkeley, California, USA

[d]Department of Plant and Microbial Biology, University of California, Berkeley, California, USA

Running Title: Integrin-Independent KSHV Infection

#Address correspondence to Laurent Coscoy, lcoscoy@berkeley.edu

ABSTRACT Host receptor usage by KSHV has been best studied using endothelial and fibroblast cells in tissue culture. In these models, KSHV adheres to the cell though heparan sulfate (HS) binding, then interacts with a complex of EphA2, xct, and integrins α3β1, αVβ3, αVβ5 to catalyze viral entry. We dissected this receptor complex at the genetic level with CRISPR-Cas9 to precisely determine receptor usage in two epithelial cell lines. Surprisingly, we discovered an infection mechanism that requires HS and EphA2, but is independent of integrin expression. Furthermore, infection appears to be independent of EphA2 signaling, despite the reliance on clathrin-mediated endocytosis. We also demonstrated while two other endogenous Eph receptors were dispensable for infection, transduced EphA4 and EphA5 significantly enhanced KSHV infection of cells lacking EphA2.

IMPORTANCE Our data reveals an integrin-independent endocytic route of KSHV infection and suggests that multiple Eph receptors besides EphA2 can promote and regulate infection. Since integrins and Eph receptors are large protein families with diverse expression patterns across cells and tissues, we propose that KSHV may engage with several proteins from both families in different combinations to negotiate successful entry into diverse cell types.

48 **INTRODUCTION**

49

50 The rhadinovirus Kaposi's Sarcoma-Associated Herpesvirus (KSHV) is one of only a handful of human
51 viruses that cause cancers. In the pathogenic state, KSHV infects and transforms endothelial cells to
52 form Kaposi's Sarcoma (KS) tumors which are particularly aggressive in the context of AIDS (1). KSHV can
53 also transform infected B cells to cause Primary Effusion Lymphoma and Multicentric Castleman's
54 Disease (2, 3), and has been linked to an inflammatory disorder (KICS) (4, 5). Although treatment with
55 antiretroviral therapy (ART) often leads to resolution of KSHV-related cancers, sudden onset of KS has
56 been recognized as a serious outcome of immune reconstitution inflammatory syndrome (KS-IRIS)
57 following ART (6, 7), and there has been little progress toward controlling KS and KSHV lymphomas in
58 endemic cases.

59

60 In the decades since its discovery, it has been observed that KSHV has broad tropism and can efficiently
61 infect many types of human primary cells and cell lines (8-10). Two of the most well-studied targets of
62 KSHV infection are endothelial cells and fibroblasts, which were of particular interest to understand the
63 origin of the transformed spindle cells that make up the distinct, highly vascularized KS tumors. Infection
64 of monocytes and dendritic cells has also been observed within KS tumors and in tissue culture models
65 (11-13). B cells are the latently infected reservoir of KSHV (14, 15), but modeling their infection in a
66 laboratory setting has proven to be technically challenging.

67

68 However, it is reasonable to assume that the first cells infected in a new host upon transmission are
69 epithelial cells. While KSHV was first considered to be a sexually transmitted infection because of its co-
70 infection pattern with HIV, it is now widely recognized that KSHV can be transmitted through saliva and
71 close contact between individuals (reviewed in 16). Multiple studies have shown that KSHV infects

72 primary human epithelial cells and cell lines including oral keratinocytes (8, 10, 17-20) and another
73 clinical report provides compelling clinical evidence that infection of the tonsillar epithelium could
74 provide a gateway through which the virus might access the underlying lymphocytes to establish the
75 reservoir of latently infected B cells (21).
76
77 KSHV interacts with a variety of receptors on the surface of host cells. Heparan sulfate (HS) is a major
78 cell attachment factor and several KSHV glycoproteins have HS-binding activities (22-28). KSHV also
79 coordinates a complex of integrins α3β1, αVβ3, αVβ5, erythropoietin-producing hepatocellular (Eph)
80 receptor A2 (EphA2), and SLC7A11/xct to trigger clathrin-mediated endocytosis or macropinocytosis of
81 the virion in fibroblasts and endothelial cells, respectively (most recently reviewed in 29, 30). In these
82 two well-characterized infection models, the interaction between KSHV gB and integrins initiates a
83 signaling cascade of FAK, Src, and PI-3K (29, 31-33). KSHV gH/gL binds EphA2 which amplifies this
84 cascade and coordinates endocytosis effectors together with c-Cbl and myosin IIA (34-37). Still, there are
85 important differences in the infection mechanisms of these model cell lines, hinting that KSHV initiates
86 different entry processes in different types of cells while using the same receptors.
87
88 In this study, we used CRISPR-Cas9 to comprehensively examine the use of this KSHV receptor complex
89 in two highly infectible epithelial cell lines: Caki-1 kidney epithelial cells, and HeLa cervical epithelial
90 cells. Caki-1 cells are significant as they have contaminated all known stocks of the SLK cell line used in
91 KSHV research (38). We found that HS and EphA2 were required for infection of both Caki-1 and HeLa
92 cells, while integrins were dispensable. Interestingly, we also found that the intracellular domain of
93 EphA2 was not required for infection of these cells, despite a reliance on clathrin-mediated endocytosis.
94 Moreover, the ectopic expression of EphA5 and overexpression of EphA4 promoted infection in *EPHA2*
95 knock out (KO) cells, but knock out of endogenous EphA4 lead to an elevated infection rate in both WT

96 and *EPHA2* KO contexts. Our studies revealed a novel integrin-independent KSHV infection mechanism
97 and suggest that Eph receptors play more diverse and complex roles during infection than was
98 previously known.
99

100 **RESULTS**

101

102 **Caki-1 and HeLa cells express most known KSHV receptors.** It has been shown that KSHV uses a
103 multimolecular complex of attachment molecules and receptors, including HS, EphA2, xct, DC-SIGN (in
104 some immune cells), and the integrin heterodimers α3β1, αVβ3, and αVβ5, to enter cells in several
105 different infection models (29). The expression of these known KSHV receptors on the surface of Caki-1
106 and HeLa cells was examined by flow cytometry. As expected, most of the KSHV receptors were
107 expressed on the surface of both cell lines: EphA2, HS, and integrin subunits α3, αV, β1, and β5 (Fig. 1).
108 Integrin β3 was additionally detected on the surface of Caki-1 cells but not HeLa cells (Fig. 1). However,
109 neither the myeloid cell marker DC-SIGN nor xct were detected on the surface of either cell line (Fig. 1).
110

111 **Heparan sulfate is necessary for KSHV infection of Caki-1 and HeLa cells.** The role of HS in adhering
112 virions to the cell surface and promoting viral entry is well documented across many virus families. Caki-
113 1 and HeLa cells express HS on the cell surface and we expected this proteoglycan to play a major role
114 during KSHV infection. We have previously shown that a deficiency in the enzyme Ext1 rendered cells
115 unable to synthesize HS (40), so we could use *EXT1* KO cells to confirm the requirement for HS during
116 KSHV entry.
117

118 An *EXT1*-specific guide sequence was cloned into px330, a Cas9 and sgRNA delivery plasmid, which was
119 then transfected into both Caki-1 and HeLa cells (Table 1). After four days, a subpopulation of HS-low

120 mutant cells was discernable by flow cytometry. The mutant population was purified by fluorescence-
121 activated cell sorting (FACS), then passaged until the immunostaining of HS in the pool decayed to
122 isotype levels (Fig. 2A). In HeLa cells, the mutant population was left unpurified from the transfected
123 pool (Fig. 2D).
124
125 The purified *EXT1* KO Caki-1 pool, WT Caki-1 cells, and the mixed *EXT1* KO HeLa pool were infected with
126 KSHV.BAC16 which encodes a constitutive GFP reporter (41), and the infection percentage was
127 quantified by measuring GFP+ cells by flow cytometry after two days. The infected mixed *EXT1* KO HeLa
128 pool was additionally stained for HS to differentiate the mutant and WT populations. As expected, the
129 infection rate of HS-deficient cells was drastically reduced compared to WT cells for both cell lines (Figs.
130 2B, 2E).
131
132 As an orthogonal approach, we used soluble heparin to competitively block KSHV infection, as this has
133 been used extensively to investigate HS usage in a variety of cell types (22, 25, 42, 43). Purified virus was
134 pre-incubated with increasing concentrations of heparin and then used to infect Caki-1 cells. Similar to
135 our results using CRISPR-Cas9 KO cells, soluble heparin inhibited infection in a dose-dependent manner
136 but approached a non-zero asymptote (Fig. 2C). Collectively, these findings confirm that HS is required
137 for efficient infection of both Caki-1 and HeLa cells, and underscores the value of CRISPR-Cas9 to study
138 viral receptor usage.
139
140 **KSHV infection of Caki-1 and HeLa cells is independent of KSHV-associated integrins.** KSHV coordinates
141 several integrin heterodimers to initiate signaling events that are required for infection of fibroblasts
142 and endothelial cells (29). Because we observed the expression of all proposed integrin receptors for
143 KSHV at the surface of Caki-1 and all, except integrin β3, on the surface of HeLa cells (Fig 1), we

144 investigated whether these integrins were required for KSHV to infect these cell lines. Both the α and β
145 subunits contribute to the unique ligand-binding surface of a given integrin heterodimer. Therefore, we
146 reasoned that the infection rates of cells with reciprocal subunits of KSHV-associated integrins knocked
147 out would reveal precisely which heterodimers were required for infection.
148
149 Single KO pools of integrins α3, αV, β1, β3, and β5 were created by transfection of Caki-1 cells with
150 px330 plasmids containing guide sequences that targeted the genes encoding each integrin subunit
151 (Table 1). The mutant populations were purified as described for *EXT1* to generate integrin KO Caki-1
152 pools (Fig. 3A). Lacking integrin αV protein, *ITGAV* KO cells lost the ability to adhere to tissue-culture
153 treated polystyrene dishes, but normal morphology and growth returned when they were plated on
154 fibronectin-coated plates. The *ITGAV* KO cells were grown on fibronectin for passaging and infection
155 experiments. The infection rates of both WT Caki-1 and HeLa cells were unchanged in the presence of a
156 fibronectin coat (data not shown). Unpurified, mixed KO HeLa cell pools were generated for integrins β1
157 and αV as described for *EXT1* (Fig. 3G). The mixed *ITGAV* KO HeLa pool was also grown on fibronectin.
158
159 WT Caki-1, the single integrin KO Caki-1 pools, and the mixed integrin KO HeLa cell pools were then
160 infected with KSHV. The mixed KO HeLa pools were additionally stained for the appropriate integrin at
161 the cell surface to allow for gating on WT and KO subpopulations. Overall, the infection rates of the
162 integrin KO pools or subpopulations were not significantly reduced compared to that of WT cells for
163 both cell lines (Fig. 3B, 3H). The slight decline in infection rate of the *ITGAV* KO HeLa subpopulation
164 compared to the WT subpopulation reached statistical significance, but the magnitude of difference was
165 similar to the other integrin KO Caki-1 pools. These data suggest that KSHV infection of Caki-1 and HeLa
166 cells does not require integrin α3β1, αVβ3, or αVβ5 alone, or any other single integrin in the αV and β1
167 families.

168

169 Although targeting single integrins has yielded clear infection defects in past studies (31, 44-46), we
170 considered that our strategy of knocking out individual integrin subunits would not reveal fully
171 redundant involvement of α3β1, αVβ3, and αVβ5 during infection of Caki-1 cells. To address this, an
172 *ITGA3/ITGAV* double KO Caki-1 pool was generated to effectively remove integrin α3β1 and the entire
173 integrin αV family, including αVβ3 and αVβ5, from the cell surface (Fig. 3C). WT and *ITGA3/ITGAV*
174 double KO Caki-1 cells were then infected with KSHV. Still, the infection rate of *ITGA3/ITGAV* double KO
175 Caki-1 cells was not reduced compared to WT cells and was in fact significantly elevated (Fig. 3D). These
176 results further indicate that integrins α3β1, αVβ3, and αVβ5 are not required for KSHV infection of Caki-
177 1 cells.

178

179 A non-RGD-binding integrin, α9β1, has been shown to bind a disintegrin-like domain (DLD) in KSHV gB
180 and is important for infection of model fibroblast and endothelial cells (47). Our data demonstrate that
181 KSHV infection of Caki-1 and HeLa cells is independent of the twelve β1-containing integrins, however
182 we considered that other integrins could still be required for KSHV infection of Caki-1 cells. There are
183 eight integrins that do not contain the αV or β1 subunits: αIIbβ3, α6β4, α4β7, αEβ7, and four β2-
184 containing integrins (Fig. 3F). Neither integrin α6, nor integrin β2 were detected on the surface of WT
185 Caki-1 cells by flow cytometry (Fig. 3E). Additionally, integrin β3 was lost from the cell surface of *ITGAV*
186 KO Caki-1 cells implying that the αIIb subunit is not available to form integrin αIIbβ3 (Fig. 3E).

187

188 We also examined the expression of all known integrin subunits in an RNA sequencing dataset from
189 iSLK.219 cells (C. Arias, personal communication), a SLK/Caki-1 cell line latently infected with KSHV, to
190 identify additional integrins that may be expressed (38, 48). The expression calls from this dataset
191 corroborated all of the flow cytometry data that was collected from WT Caki-1 cells in this study (Fig.

192 3F). Surprisingly, the αE subunit appeared to be expressed in the RNA-seq dataset, but not the conjugate
193 β7 subunit (Fig. 3F). Altogether the data from these two approaches indicate that none of the eight non-
194 αV, non-β1 integrins are expressed in Caki-1 cells, so these integrins are unlikely to play a role in this
195 KSHV infection mechanism.
196
197 **EphA2 is necessary for KSHV infection of Caki-1 and HeLa cells.** EphA2 has been well-characterized as a
198 receptor for KSHV and binds to the envelope glycoprotein complex gH/gL (37, 49, 50). Together with
199 integrins, EphA2 helps propagate virus-induced signaling and mobilize endocytosis effectors which leads
200 to viral entry in multiple cell types (34-36, 49, 51, 52). However, we found that KSHV infection of Caki-1
201 and HeLa cells does not require integrins, so we investigated whether EphA2 was required for infection
202 in these cell lines.
203
204 Caki-1 cells were transfected with a px330 plasmid containing a guide sequence targeting *EPHA2* and an
205 *EPHA2* KO pool was isolated as described for *EXT1* (Fig. 4A). In addition, a mixed WT/*EPHA2* KO pool was
206 generated in HeLa cells as described for *EXT1* (Fig. 4D). WT and *EPHA2* KO Caki-1 cells and the mixed
207 WT/KO HeLa pool were then infected with KSHV. The mixed WT/KO HeLa pool was additionally stained
208 for surface EphA2 expression to distinguish the KO and WT subpopulations. *EPHA2* KO cells were
209 significantly less susceptible to infection compared to WT cells in both cell lines, though they were not
210 completely resistant to the virus (Figs. 4B, 4E). These results indicate that EphA2 is necessary for
211 efficient infection of both Caki-1 and HeLa cells.
212
213 A prior study demonstrated that KSHV gH/gL has the ability to bind other Eph receptors besides EphA2
214 in multiple assays (50). We hypothesized that the residual KSHV infection of *EPHA2* KO cells could
215 depend on other Eph receptors that may be expressed by Caki-1 cells. To test whether this was the case,

216 *EPHA2* KO cells were pre-incubated with either soluble ephrin-A4-Fc or EGFR-Fc chimeric proteins, then
217 infected with KSHV in the presence of these blocking agents. The infection rate of *EPHA2* KO cells was
218 further reduced in the presence of ephrin-A4-Fc compared to the unrelated EGFR-Fc (Fig. 4C). Since
219 ephrin ligands, including ephrin-A4, can broadly bind to and block interactions with Eph receptors of the
220 same type, these data suggest that another A-type Eph receptor is expressed by Caki-1 cells and
221 required for infection in the absence of EphA2.
222
223 **EphA4 and EphB2 are dispensable for KSHV infection in Caki-1 cells.** Since we found that residual
224 infection in *EPHA2* KO Caki-1 cells could be further blocked by a soluble ephrin ligand, we investigated
225 whether additional Eph receptors were expressed by Caki-1 cells and if they were required for KHSV
226 infection of Caki-1 cells. EphA4 and EphB2 transcripts were found in the RNA sequencing dataset from
227 iSLK.219 cells (C. Arias, personal communication) and we confirmed the expression of these two
228 proteins by western blot (Figs. 5E, 5H).
229
230 WT Caki-1 cells were transfected with px330 plasmids containing guide sequences targeting *EPHA4* and
231 *EPHB2* (Table 1). We were unable to find an antibody that reliably detected EphA4 or EphB2 by surface
232 immunostaining of live cells, so single-cell clones were derived from the transfected populations and
233 screened for loss of EphA4 or EphB2 by western blot. Two *EPHA4* KO Caki-1 cell lines and one *EPHB2* KO
234 Caki-1 cell line were isolated (Figs. 5A, 5F). WT, *EPHA4* KO, and *EPHB2* KO Caki-1 cell lines were then
235 infected with KSHV. Surprisingly, the infection rate of *EPHA4* KO cells was elevated compared to WT
236 cells, while the infection rate of *EPHB2* KO cells was unchanged (Figs. 5B, 5G). The same results were
237 observed in *EPHA4* and *EPHB2* KO Caki-1 cell pools created with a lentiviral CRISPR-Cas9 system (data
238 not shown).
239

240 To further understand the infection phenotype of *EPHA4* KO cells, one of the *EPHA4* KO Caki-1 cell lines
241 was transfected with the *EPHA2*-targeted px330 plasmid (Table 1) and a pool of *EPHA2/EPHA4* DKO cells
242 was isolated by FACS (Figs. 5A, 5D). When these cells were infected with KSHV, the infection rate was
243 reduced compared to WT cells, but significantly elevated compared to *EPHA2* single KO cells (Fig. 5C).
244 These data indicate that either EphA4 is a negative regulator of KSHV infection, or that Caki-1 cells
245 compensate for the loss of EphA4 in a way that enhances KSHV infection.
246
247 EphA4 and EphB2 were detected in Caki-1 lysate and EphA4 was additionally found in 293T lysate.
248 Importantly, both of these proteins were lacking in HeLa cell lysate, even though EphA2-independent
249 infection was observed in both Caki-1 and HeLa cells (Figs. 5E, 5H). Furthermore, these results show that
250 EphA4 and EphB2 are dispensable for KSHV infection and are unlikely to be the functional targets of
251 ephrin-A4-Fc blocking during infection of *EPHA2* KO Caki-1 cells.
252
253 **Multiple Eph receptors rescue KSHV infection of EphA2 KO cells**. Although we found that two
254 endogenous Eph receptors besides EphA2 were not required for KSHV infection in WT Caki-1 cells, the
255 significant infection defect of EPHA2 KO Caki-1 cells provided an ideal platform to test the effects of
256 transduced Eph receptors on KSHV infection. A clonal EphA2 KO Caki-1 cell line was isolated from single-
257 cell clones of the EphA2 KO pool and was used for the remainder of the experiments. The clone lacked
258 surface expression of EphA2 and the infection defect compared to WT cells was similar to the parent
259 population (Fig. 6F).
260
261 To ensure that expression levels of different Eph receptors could be compared, mature forms of *EPHA2*,
262 *EPHA4*, and *EPHA5* lacking endogenous signal peptides were cloned into p3xFlag-CMV-9 following the
263 preprotrypsin leader sequence and a 3xFlag tag (Fig. 6A). This cloning scheme ensured that the proteins

264 would be properly oriented in the membrane during translation and ultimately be N-terminally tagged
265 with 3xFlag. The 3xFlag-tagged Eph receptor constructs were cloned into a retroviral vector and
266 transduced into *EPHA2* KO Caki-1 cells.
267
268 The 3xFlag tag was detected on the surface of each cell line by flow cytometry, although the magnitude
269 of expression varied with each receptor (Fig. 6B). However, when the cell lines were stained for
270 intracellular 3xFlag, the overall expression levels of the receptors appeared to be similar to each other
271 (Fig. 6D). Additionally, when the expression of the receptors was examined by western blot, the
272 intensities of the 3x-Flag-tagged bands were similar across the three transduced cell lines (Fig. 6C).
273 These data show that all three constructs were expressed to a similar degree but that cell surface
274 trafficking of the three receptors was differentially regulated.
275
276 The expression of the 3x-Flag-tagged Eph receptors was also compared to the corresponding
277 endogenous protein. The peak of surface expression of transduced 3xFlag-EphA2 was slightly higher
278 than endogenous EphA2 as measured by flow cytometry, but the range of EphA2 expression in the
279 population of 3xFlag-EphA2-transduced cells was much greater compared to WT cells (Fig. 6E). EphA5
280 was not naturally expressed by Caki-1 cells, but EphA5 was readily detected in 3xFlag-EphA5-transduced
281 cells as a wide peak by flow cytometry and also as a strong band by western blot (Figs. 6E, 6D). In
282 contrast, EphA4 was found to be expressed endogenously by Caki-1 cells by western blot and the EphA4
283 band became more pronounced in the 3xFlag-EphA4-transduced cell lysate (Fig. 6D).
284
285 WT Caki-1, *EPHA2* KO Caki-1, and the 3xFlag-tagged Eph receptor transduced *EPHA2* KO cell lines and a
286 vector control were infected with KSHV. The surface 3xFlag expression was measured concurrently with
287 infection rate by flow cytometry. 3xFlag-EphA2, 3xFlag-EphA4, and 3xFlag-EphA5 all significantly rescued

288 the infection rate to varying degrees compared to the vector control (Fig. 6F). Because of the broad
289 range of flag-tagged receptor expression within the populations of the transduced cell lines, we also
290 examined how the infection rate changed with surface protein level. The histograms of 3xFlag
291 expression from one replicate well of the experiment were divided into five successive gates (Fig. 6G).
292 The percent GFP+ cells in each bin was plotted against the fold geometric mean of the fluorescence
293 intensity (MFI) over isotype MFI of each bin (Fig. 6G). Surprisingly, we found that both EphA4 and EphA5
294 mediated higher KSHV infection rates at lower amounts of surface protein compared to EphA2.
295 However, at very high surface expression levels that were only attained by EphA2, the infection rate
296 surpassed that of WT cells from the same experiment (Fig. 6F).
297
298 Altogether these data show that EphA2, EphA4 and EphA5 can rescue the infection rate phenotype of
299 *EPHA2* KO cells which suggests that the function of EphA2 in this infection mechanism may not be
300 specific to EphA2. Moreover, the overexpression of EphA4 in this context strongly enhanced KSHV
301 infection, which is not what we expected based on our *EPHA4* KO experiments. The precise role of
302 endogenous EphA4 cannot be discerned from these studies alone.
303
304 **Ectodomain of EphA2 is sufficient to rescue KSHV infection in EphA2 KO cells.** In endothelial and
305 fibroblast KSHV infection models, several studies have reported that downstream effector proteins co-
306 immunoprecipitate and colocalize with EphA2, implying involvement of the cytoplasmic tail of EphA2
307 which contains a kinase and several protein-protein interaction domains (34-36, 51). Here we have
308 shown that KSHV infection of Caki-1 and HeLa cells is independent of integrins, but still dependent on
309 EphA2. Eph receptors can naturally trigger endocytosis in response to ephrin ligand binding by several
310 mechanisms (reviewed in 53). Since KSHV gH/gL binds to the ephrin-binding domain of EphA2 (37), we

311 hypothesized that the signaling domains in the cytoplasmic tail of EphA2 would be necessary for
312 infection and would provide clues about how the virus might use EphA2 to enter cells without integrins.
313
314 To this end, a truncation mutant of EphA2 was generated which lacked all cytoplasmic signaling
315 domains. This cytoplasmic truncation (ΔCT) contained the entire peptide signal and ectodomain (amino
316 acids 1-537) and the transmembrane (TM) domain (aa 538-558) (Fig. 7A). Full length *EPHA2* (FL) and
317 *EPHA2* ΔCT were cloned into retroviral vectors and stably transduced into *EPHA2* KO Caki-1 and HeLa
318 cells. Both EphA2 FL and EphA2 ΔCT were expressed on the cell surface to a slightly higher degree than
319 endogenous EphA2 on Caki-1 (Fig. 7D) and HeLa cells (data not shown). When infected with KSHV, both
320 EphA2 FL and EphA2 ΔCT significantly rescued infection to nearly identical levels compared to the vector
321 control (Figs. 7B, 7C).
322
323 Eph receptor clustering is essential for natural signaling events, and a homodimerization region has been
324 found within the transmembrane domain of EphA1 by nuclear magnetic resonance spectroscopy (54).
325 To test whether the transmembrane domain was required for EphA2 ectodomain function during KSHV
326 infection, we performed additional domain swaps with the EphA2 ΔCT construct and replaced the EphA2
327 TM domain with that of integrin β1 or HLA-B7, two unrelated single-pass transmembrane proteins (Fig.
328 7A). These domain-swapped constructs were also cloned into retroviral vectors and transduced into
329 *EPHA2* KO Caki-1 cells. The EphA2/HLA-B7 chimeric CT and EphA2/integrin β1 chimeric ΔCT constructs
330 were expressed at the cell surface to the same degree as the FL and CT constructs, and they also
331 significantly rescued KSHV infection of *EPHA2* KO cells (Figs. 7D, 7B). Together, these data show that
332 only the ectodomain of EphA2 is required to rescue KSHV infection in *EPHA2* KO Caki-1 cells.
333

334 **KSHV requires dynamin and clathrin to infect Caki-1 and HeLa cells.** It is well-known that clathrin-
335 mediated endocytosis and lipid raft-dependent micropinocytosis are the routes of virion internalization
336 triggered by KSHV-receptor interactions in fibroblasts and endothelial cells, respectively (reviewed in
337 29). In this study we have discovered an infection mechanism that does not seem to use the same KSHV-
338 induced integrin/EphA2 signaling axis that has been characterized in these types. However, we
339 hypothesized that endocytosis would still be a necessary step of this novel infection mechanism
340 regardless of how it was induced.
341
342 Chlorpromazine, dynasore, and nystatin were each tested for their ability to inhibit KSHV infection of
343 both WT and *EPHA2* KO Caki-1 cells and HeLa cells. Chlorpromazine disrupts the assembly of clathrin
344 coated vesicles at the cell surface and dynasore inhibits the activity of dynamin which is required for
345 newly formed endocytic vesicles to pinch off from the plasma membrane. Nystatin sequesters
346 cholesterol and disrupts lipid raft structures. Cells were pre-treated with the indicated concentrations of
347 these three drugs, then infected with KSHV while drug concentrations were maintained. In all three cell
348 lines, we found that chlorpromazine and dynasore significantly reduced KSHV infection (Fig. 8). These
349 data suggest that KHSV infection in all three cell lines requires clathrin-mediated endocytosis. Notably,
350 while nystatin did not affect the infection rate in WT Caki-1 and HeLa cells, it seemed to enhance
351 infection of *EPHA2* KO Caki-1 cells (Fig. 8B).
352
353 **DISCUSSION**
354
355 In this report, we describe a novel KSHV infection mechanism in Caki-1 and HeLa cells which requires HS
356 and the ectodomain of EphA2 but is independent of integrins. We also present compelling evidence that

357 EphA4 and EphA5 may regulate KSHV infection in various contexts. CRISPR-Cas9 proved to be a valuable
358 tool to dissect the roles of individual receptors during KSHV infection.
359
360 Surprisingly, we found that KSHV infection was completely unaffected by perturbations in the integrin
361 network in Caki-1 and HeLa cells. Cells lacking expression of both integrin subunits α3 and αV, effectively
362 lacking all three known KSHV integrin receptors, were even infected at a slightly higher rate compared
363 to WT cells. Our CRISPR-Cas9 KO studies covered sixteen of the twenty-four known integrin
364 heterodimers, and we further determined that the remaining eight heterodimers were not expressed in
365 Caki-1 cells.
366
367 This result was unexpected because studies in endothelial and fibroblast cells have demonstrated a
368 requirement for some combination of the integrins α3β1, αVβ3, or αVβ5 for productive KSHV entry
369 (reviewed in 29), although there has been some dispute about exactly which integrins are necessary (44,
370 46, 55, 56). It is still conceivable that an αV-family and one or more β1-family integrins besides α3β1 are
371 fully redundant receptors of KSHV in this system, although such a situation would not be consistent with
372 several past studies where a KSHV infection phenotype was recorded after targeting only a single
373 integrin heterodimer with a blocking antibody (31, 44, 45).
374
375 The KSHV glycoprotein gB binds integrins through an RGD domain that mimics natural integrin ligands,
376 as well as a DLD domain (31, 44, 47, 57). This gB-integrin interaction is required to initiate the KSHV-
377 induced signaling cascade through the activation of focal adhesion kinase and other downstream
378 effectors that eventually lead to virion endocytosis (31-33). This leads to the outstanding question of
379 how KSHV initiates endocytosis in Caki-1 and HeLa cells without the involvement of integrins. In known
380 infection mechanisms, the cytoplasmic domain of EphA2 is essential to propagate KSHV-induced

381 signaling events and recruit effectors of macropinocytosis and clathrin-mediated endocytosis (34-36,
382 51). We hypothesized that KSHV might directly induce endocytosis through EphA2, mimicking natural
383 ephrin ligand-receptor binding events (37). While we found that infection of Caki-1 and HeLa cells
384 required EphA2, remarkably an EphA2 construct truncated after the TM domain rescued infection in
385 *EPHA2* KO cells as efficiently as the full-length EphA2 construct.
386
387 Together, our results suggest that in Caki-1 and HeLa cells, KSHV does not trigger the same integrin-
388 EphA2 signaling axis that is so crucial for entry into endothelial cells and fibroblasts. However, this
389 conclusion must be rectified with the strong infection defect we observed in *EPHA2* KO cells. The KSHV
390 membrane glycoprotein gH/gL binds to EphA2 (37, 49, 50), so one interpretation of our data is simply
391 that the ectodomain of EphA2 acts as an adhesion receptor in this setting. It may also play a role in
392 localizing virions and/or receptors to membrane microdomains that subsequently promote virion
393 endocytosis, as we observed an increased KSHV infection rate upon lipid raft disruption by nystatin
394 treatment in *EPHA2* KO cells but not WT cells, while the sensitivity to clathrin and dynamin inhibitors
395 remained consistent.
396
397 Taken together with our experiments investigating potential roles for different Eph receptors during
398 KSHV infection, more speculative hypotheses can also be made. The result that we were able to further
399 inhibit infection of *EPHA2* KO cells with ephrin-A4 suggests that another factor which is blocked by
400 ephrin-A4, most likely an Eph receptor, promotes KSHV infection. We ruled out that endogenous EphA4
401 and EphB2 were necessary for infection of Caki-1 infection, but also found that these Eph receptors
402 were not expressed by HeLa cells. This is important because like Caki-1 cells, HeLa cells exhibit a
403 significant amount of EphA2-independent KSHV infection. It is possible that additional Eph receptors are
404 expressed by both cell lines and affect KSHV infection in *EPHA2* KO and WT contexts.

405

406 In support of this idea, we demonstrated that transduced EphA4 and EphA5 constructs rescued infection
407 rates in *EPHA2* KO cells to levels comparable with transduced EphA2. In fact, at low amounts of surface
408 expression, EphA4 and EphA5 constructs outperformed EphA2 in this assay. It is unclear why EphA4 is
409 dispensable for infection in the endogenous setting, while it promoted KSHV infection in this context.
410 Spliced or modified forms of EphA4 produced from the endogenous gene could account for this
411 discrepancy. Alternatively, EphA4 may be part of a homeostatic network that ultimately impacts KSHV
412 infection efficiency and cellular adaptation to the loss of EphA4 could be responsible for the KO
413 phenotype. Whether EphA4, EphA5, and other Ephs act as true cellular receptors for KSHV should be
414 further investigated.

415

416 A striking property of Eph receptors is that they form heterotetramers with their ligands as well as large
417 oligomerized arrays through Eph-Eph interactions in their ectodomains which are critical to trigger
418 forward signaling in response to ligands (58-61). These signaling arrays can contain multiple types of Eph
419 receptors, Eph receptors that are not bound to ligands, and Eph receptor ectodomains (58, 59, 61-63).
420 Moreover, Eph cluster size, composition, and the presence of alternatively spliced Eph receptor forms
421 may all influence the cellular outcomes of Eph signaling (64-66). Importantly, one study showed that the
422 ectodomain of EphA2 was sufficient to localize the protein to cell-cell contacts (58), and another study
423 of chimeric EphA2 and EphA4 constructs suggested that the ectodomain may be a stronger determinant
424 of cellular responses than the attached cytoplasmic domain (60).

425

426 Thus, it is conceivable that in the presence of other signaling-competent Eph receptors, the ectodomain
427 of EphA2 could promote clustering and signaling during KSHV infection just as well as the full-length
428 receptor as we observed in our experiments. However, it is also possible that an unknown factor—not

429 an Eph receptor—is responsible for virion endocytosis and EphA2-independent infection in Caki-1 and
430 HeLa cells.
431
432 Given the importance of epithelial cell infection for host colonization, it will be valuable to further
433 characterize this infection mechanism and its impact on the viral life cycle. Our data support the notion
434 that KSHV receptor usage and entry mechanisms vary between cell types. We propose that KSHV
435 infection is not restricted by integrin and EphA2 expression and that the virus may utilize several
436 members of both the integrin and Eph receptor families in various combinations for entry into a broad
437 variety of cell types throughout the body. Modern gene editing technologies such as CRISPR-Cas9 will
438 facilitate detailed studies of KSHV receptors in the future and have the potential to rapidly expand the
439 field of virus-host interactions.
440

441 **MATERIALS AND METHODS**
442

443 **Cell lines and culture.** SLK/Caki-1 (ATCC HTB-46) cells were a gift from D. Ganem. HeLa cells (ATCC CCL-
444 2) were obtained from the UC Berkeley BDS Cell Culture Facility. 293T (ATCC CRL-1573) and Phoenix
445 (ATCC CRL-3213) cells were purchased from the ATCC. Cells were grown in high glucose Dulbecco's
446 Modified Eagle's Medium (DMEM, Gibco) supplemented with 5% fetal bovine serum (FBS, SeraDigm) at
447 37°C with 5% CO_2.
448

449 **KSHV production and infection.** iSLK.Bac16 (gift from J. Jung, USC) cells harboring latent KSHV.BAC16
450 infection were cultured under selection with 1.2 mg/mL of hygromycin B (Invitrogen). The cells were
451 induced to produce virus with 1 mM sodium butyrate (Alfa Aesar) and 1 ug/mL doxycycline (Sigma-
452 Aldrich). Three days after reactivation, supernatant was collected and filtered through a 0.45 µm syringe
453 filter. The unconcentrated viral supernatant was stored at 4°C and diluted with standard culture medium

454 for use in infection experiments. The dilution was calculated for each batch to produce an approximate
455 infection rate of 30% on WT Caki-1 cells, measured in GFP+ events by flow cytometry. Cells were
456 incubated with virus for 12-24 hours, then viral supernatant was removed and replaced with fresh
457 medium until analysis two days post infection.
458
459 **CRISPR-Cas9 genome editing.** Guide sequences were designed using the online tool crispr.mit.edu and
460 are provided in Table 1. A 5' G was added to sequences that didn't already contain one and then the
461 appropriate adaptors were appended to both forward and reverse oligos to facilitate cloning into px330
462 (Addgene #42230) according to the protocol provided at genomeengineering.org. Assembled px330
463 plasmids were transfected into cells of interest and mutant cells were sorted by FACS or subcloned to
464 obtain genetic KO cell pools or cell lines, respectively.
465
466 **Antibodies.** Heparan sulfate antibody (F58-10E4) was purchased from Amsbio, integrin α3 antibody
467 (P1B5 from Calbiochem, integrin αV and EphA5 antibodies (MAB12191 and MAB541, respectively) from
468 R&D Systems, integrin β1 and integrin β3 antibodies (T2S/16 and PM6/13, respectively) from Novus
469 Biologicals, integrin β5 and EphA2 antibodies (AST-3T and SHM16, respectively) from BioLegend, xct and
470 GAPDH antibodies (ab37185 and ab181602, respectively) from Abcam, DC-SIGN antibody (DCN47.5)
471 from Miltenyi Biotec, EphA4 antibody (4C8H5) from ThermoFisher, EphB2 antibody (2D12C6) from Santa
472 Cruz Biotech, and Flag antibody (M2) from Sigma-Aldrich. Purified isotype control antibodies (MAB002,
473 MAB003, MAB004, AB-105-C, MAB006) were purchased from R&D Systems except mouse IgM, κ (MM-
474 30) was from BioLegend.
475
476 **Endocytosis Inhibitors.** Cells were pretreated with Chlorpromazine (Chem-Impex), Dynasore (Sigma-
477 Aldrich), or Nystatin (Chem-Impex) for 30 minutes. Following pretreatment, cells were infected with

478 KSHV for 4 hours while maintaining the indicated drug concentration. Cells were washed and infection
479 rate was measured two days later.
480
481 **Ephrin-A4 Blocking.** Cells were preblocked with ephrin-A4-Fc or EGFR-Fc (R&D Systems) for 30 minutes
482 prior to infection at the indicated concentration, then virus was added in a 1:1 volume ratio and the cells
483 were infected overnight. The cells were then washed, given fresh culture medium, and grown for one
484 additional day before analyzing infection rate.
485
486 **Constructs and Cloning.** Eph receptors were amplified from BJAB (EphA4, EphA5) or Caki-1 (EphA2)
487 cDNA and directly cloned into pQCXIN (Clontech) or cloned into p3xFlag-CMV-9 (Sigma-Aldrich) and
488 subsequently cloned into pQCXIN to add an N-terminal 3xFlag tag preceded by the preprotrypsin leader
489 sequence. Truncation mutants were amplified with a reverse primer in the indicated position containing
490 an artificial stop codon. Chimeric TM domain EphA2 constructs were made using SOEing PCR.
491
492 **Transfection and Transduction.** Caki-1 and HeLa cells were transfected with px330 and phoenix cells
493 were transfected with pQCXIN-based constructs using Fugene transfection reagent (Promega) and
494 Optimem (Gibco) according to the manufacturer's instructions. After 2-3 days, retrovirus was collected
495 from the phoenix cell supernatant and filtered through a 0.45 µm filter. Filtered retroviral supernatant
496 was applied to target cells with 6 µg/mL polybrene (Santa Cruz) and spinfected at 500x g for 2 hours at
497 room temperature. Transduced cells were selected with neomycin (Fisher Scientific) at 1.2 mg/mL.
498
499 **Flow Cytometry and Sorting.** Cells were harvested with trypsin (Gibco) or PBS (Gibco) + 2 µM EDTA
500 (Fisher) when staining for trypsin-sensitive epitopes. Cells were blocked, stained, and washed in 1% BSA
501 (Fisher) in PBS. When applicable, cells were fixed in 4% PFA (ThermoFisher Pierce) in PBS and

502 permeabilized with 0.25% Triton X-100 (EM Science) in PBS. Live cells were stained with DAPI
503 (BioLegend) and fixed cells with Ghost Dye Violet 510 (Tonbo Biosciences) for viability according to the
504 manufacturer's instructions. Cells were analyzed using an LSR Fortessa or LSR Fortessa X-20 cell analyzer
505 (BD Biosciences) and sorted using a BD Influx or BD FACSARIA Fusion cell sorter (BD Biosciences). Data
506 was processed and visualized with FlowJo 10 (BD Biosciences).
507
508 **Western Blotting.** Cells were harvested by scraping in PBS and lysed in RIPA buffer (150 mM sodium
509 chloride, 1% Triton X-100, 0.5% sodium deoxycholate, 0.1% sodium dodecyl sulfate, 50 mM Tris, and a
510 protease inhibitor cocktail (Roche)). Protein concentration in lysate was quantified by BCA assay
511 (ThermoFisher Pierce). Lysates were run on a 10% polyacrylamide gel and transferred to a nitrocellulose
512 membrane. A buffer containing 3% BSA and 10% FBS in TBST (20 mM Tris, 150 mM sodium chloride,
513 0.1% Tween 20) was used for blocking and primary antibody incubation. Plain TBST was used for
514 washing and secondary antibody incubation. Blots were visualized with IRDye 800CW and 680RD
515 secondary antibodies from LI-COR Biosciences using a LI-COR Odyssey infrared scanner and analyzed in
516 ImageStudio Lite 5.2 (LI-COR Biosciences).
517
518 **Statistical Analysis.** The indicated data sets were compared using the student's t-test in Prism 7
519 (GraphPad). A p value < 0.05 was denoted with a *.
520
521 **ACKNOWLEDGEMENTS**
522
523 This research received no specific grant from any funding agency in the public, commercial, or not-for-
524 profit sectors. The authors would like to thank Hector Nolla and Alma Valeros from the University of
525 California, Berkeley Flow Cytometry Core Facility for technical assistance and advice and Dr. Carolina

526 Arias from University of California, Santa Barbara, for graciously sharing her RNA-seq data. The authors
527 would like to additionally thank Dr. Ellen Robey, Dr. Eva Harris, Dr. Trever Greene, Andrew Birnberg,
528 Kristina Geiger, and Valerie Vargas-Zapata for enlightening discussion about this project.

529

530 **REFERENCES**

531

532 1. Chang Y, Cesarman E, Pessin MS, Lee F, Culpepper J, Knowles DM, Moore PS. 1994.
533 Identification of herpesvirus-like DNA sequences in AIDS-associated Kaposi's sarcoma. Science
534 266:1865-1869.
535 2. Cesarman E, Chang Y, Moore PS, Said JW, Knowles DM. 1995. Kaposi's sarcoma-associated
536 herpesvirus-like DNA sequences in AIDS-related body-cavity-based lymphomas. N Engl J Med
537 332:1186-1191.
538 3. Soulier J, Grollet L, Oksenhendler E, Cacoub P, Cazals-Hatem D, Babinet P, d'Agay MF, Clauvel JP,
539 Raphael M, Degos L. 1995. Kaposi's sarcoma-associated herpesvirus-like DNA sequences in
540 multicentric Castleman's disease. Blood 86:1276-1280.
541 4. Uldrick TS, Wang V, O'Mahony D, Aleman K, Wyvill KM, Marshall V, Steinberg SM, Pittaluga S,
542 Maric I, Whitby D, Tosato G, Little RF, Yarchoan R. 2010. An interleukin-6-related systemic
543 inflammatory syndrome in patients coinfected with Kaposi sarcoma-associated herpesvirus and
544 HIV but without multicentric Castleman disease. Clin Infect Dis 51:350-358.
545 5. Polizzotto MN, Uldrick TS, Wyvill KM, Aleman K, Marshall V, Wang V, Whitby D, Pittaluga S, Jaffe
546 ES, Millo C, Tosato G, Little RF, Steinberg SM, Sereti I, Yarchoan R. 2016. Clinical Features and
547 Outcomes of Patients With Symptomatic Kaposi Sarcoma Herpesvirus (KSHV)-associated
548 Inflammation: Prospective Characterization of KSHV Inflammatory Cytokine Syndrome (KICS).
549 Clin Infect Dis 62:730-738.

550 6. Bower M, Nelson M, Young AM, Thirlwell C, Newsom-Davis T, Mandalia S, Dhillon T, Holmes P,
551 Gazzard BG, Stebbing J. 2005. Immune reconstitution inflammatory syndrome associated with
552 Kaposi's sarcoma. J Clin Oncol 23:5224-5228.
553 7. Volkow P, Cesarman-Maus G, Garciadiego-Fossas P, Rojas-Marin E, Cornejo-Juárez P. 2017.
554 Clinical characteristics, predictors of immune reconstitution inflammatory syndrome and long-
555 term prognosis in patients with Kaposi sarcoma. AIDS Res Ther 14:30.
556 8. Renne R, Blackbourn D, Whitby D, Levy J, Ganem D. 1998. Limited Transmission of Kaposi's
557 Sarcoma-Associated Herpesvirus in Cultured Cells. J Virol 72:5182-5188.
558 9. Blackbourn DJ, Lennette E, Klencke B, Moses A, Chandran B, Weinstein M, Glogau RG, Witte MH,
559 Way DL, Kutzkey T, Herndier B, Levy JA. 2000. The restricted cellular host range of human
560 herpesvirus 8. AIDS 14:1123-1133.
561 10. Bechtel JT, Liang Y, Hvidding J, Ganem D. 2003. Host Range of Kaposi's Sarcoma-Associated
562 Herpesvirus in Cultured Cells. J Virol 77:6474-6481.
563 11. Blasig C, Zietz C, Haar B, Neipel F, Esser S, Brockmeyer NH, Tschachler E, Colombini S, Ensoli B,
564 Stürzl M. 1997. Monocytes in Kaposi's sarcoma lesions are productively infected by human
565 herpesvirus 8. J Virol 71:7963-7968.
566 12. Rappocciolo G, Jenkins FJ, Hensler HR, Piazza P, Jais M, Borowski L, Watkins SC, Rinaldo CR.
567 2006. DC-SIGN is a receptor for human herpesvirus 8 on dendritic cells and macrophages. J
568 Immunol 176:1741-1749.
569 13. Rappocciolo G, Jais M, Piazza PA, DeLucia DC, Jenkins FJ, Rinaldo CR. 2017. Human Herpesvirus 8
570 Infects and Replicates in Langerhans Cells and Interstitial Dermal Dendritic Cells and Impairs
571 Their Function. J Virol 91:e00909-17.

572 14. Mesri EA, Cesarman E, Arvanitakis L, Rafii S, Moore MA, Posnett DN, Knowles DM, Asch AS.
573 1996. Human herpesvirus-8/Kaposi's sarcoma-associated herpesvirus is a new transmissible
574 virus that infects B cells. J Exp Med 183:2385-2390.
575 15. Blackbourn DJ, Ambroziak J, Lennette E, Adams M, Ramachandran B, Levy JA. 1997. Infectious
576 human herpesvirus 8 in a healthy North American blood donor. Lancet 349:609–611.
577 16. Minhas V, Wood C. 2014. Epidemiology and Transmission of Kaposi's Sarcoma-Associated
578 Herpesvirus. Viruses 6:4178-4194.
579 17. Cerimele F, Curreli F, Ely S, Friedman-Kien AE, Cesarman E, Flore O. 2001. Kaposi's Sarcoma-
580 Associated Herpesvirus Can Productively Infect Primary Human Keratinocytes and Alter Their
581 Growth Properties. J Virol 75:2435-2443.
582 18. Duus K, Lentchitsky V, Wagenaar T, Grose C, Webster-Cyriaque J. 2004. Wild-Type Kaposi's
583 Sarcoma-Associated Herpesvirus Isolated from the Oropharynx of Immune-Competent
584 Individuals Has Tropism for Cultured Oral Epithelial Cells. J Virol 78:4074-4084.
585 19. Johnson AS, Maronian N, Vieira J. 2005. Activation of Kaposi's sarcoma-associated herpesvirus
586 lytic gene expression during epithelial differentiation. J Virol 79:13769-13777.
587 20. Gong D, Wu NC, Xie Y, Feng J, Tong L, Brulois KF, Luan H, Du Y, Jung JU, Wang CY, Kang MK, Park
588 NH, Sun R, Wu TT. 2014. Kaposi's sarcoma-associated herpesvirus ORF18 and ORF30 are
589 essential for late gene expression during lytic replication. J Virol 88:11369-11382.
590 21. Chagas CA, Endo LH, Sakano E, Pinto GA, Brousset P, Vassallo J. 2006. Detection of herpesvirus
591 type 8 (HHV8) in children's tonsils and adenoids by immunohistochemistry and in situ
592 hybridization. Int J Pediatr Otorhinolaryngol 70:65-72.
593 22. Akula SM, Wang FZ, Vieira J, Chandran B. 2001. Human herpesvirus 8 interaction with target
594 cells involves heparan sulfate. Virology 282:245-255.

595 23. Akula SM, Pramod NP, Wang FZ, Chandran B. 2001. Human herpesvirus 8 envelope-associated
596 glycoprotein B interacts with heparan sulfate-like moieties. Virology 284:235-249.
597 24. Wang FZ, Akula SM, Pramod NP, Zeng L, Chandran B. 2001. Human herpesvirus 8 envelope
598 glycoprotein K8.1A interaction with the target cells involves heparan sulfate. J Virol 75:7517-
599 7527.
600 25. Birkmann A, Mahr K, Ensser A, Yağuboğlu S, Titgemeyer F, Fleckenstein B, Neipel F. 2001. Cell
601 surface heparan sulfate is a receptor for human herpesvirus 8 and interacts with envelope
602 glycoprotein K8.1. J Virol 75:11583-11593.
603 26. Mark L, Lee WH, Spiller OB, Villoutreix BO, Blom AM. 2006. The Kaposi's sarcoma-associated
604 herpesvirus complement control protein (KCP) binds to heparin and cell surfaces via positively
605 charged amino acids in CCP1-2. Mol Immunol 43:1665-1675.
606 27. Spiller OB, Mark L, Blue CE, Proctor DG, Aitken JA, Blom AM, Blackbourn DJ. 2006. Dissecting the
607 regions of virion-associated Kaposi's sarcoma-associated herpesvirus complement control
608 protein required for complement regulation and cell binding. J Virol 80:4068-4078.
609 28. Hahn A, Birkmann A, Wies E, Dorer D, Mahr K, Stürzl M, Titgemeyer F, Neipel F. 2009. Kaposi's
610 sarcoma-associated herpesvirus gH/gL: glycoprotein export and interaction with cellular
611 receptors. J Virol 83:396-407.
612 29. Kumar B, Chandran B. 2016. KSHV Entry and Trafficking in Target Cells-Hijacking of Cell Signal
613 Pathways, Actin and Membrane Dynamics. Viruses 8:305.
614 30. Kumar B, Roy A, Veettil MV, Chandran B. 2018. Insight into the Roles of E3 Ubiquitin Ligase c-
615 Cbl, ESCRT Machinery, and Host Cell Signaling in Kaposi's Sarcoma-Associated Herpesvirus Entry
616 and Trafficking. J Virol 92.

617 31. Akula SM, Pramod NP, Wang FZ, Chandran B. 2002. Integrin alpha3beta1 (CD 49c/29) is a
618 cellular receptor for Kaposi's sarcoma-associated herpesvirus (KSHV/HHV-8) entry into the
619 target cells. Cell 108:407-419.
620 32. Naranatt PP, Akula SM, Zien CA, Krishnan HH, Chandran B. 2003. Kaposi's sarcoma-associated
621 herpesvirus induces the phosphatidylinositol 3-kinase-PKC-zeta-MEK-ERK signaling pathway in
622 target cells early during infection: implications for infectivity. J Virol 77:1524-1539.
623 33. Sharma-Walia N, Naranatt PP, Krishnan HH, Zeng L, Chandran B. 2004. Kaposi's sarcoma-
624 associated herpesvirus/human herpesvirus 8 envelope glycoprotein gB induces the integrin-
625 dependent focal adhesion kinase-Src-phosphatidylinositol 3-kinase-rho GTPase signal pathways
626 and cytoskeletal rearrangements. J Virol 78:4207-4223.
627 34. Chakraborty S, Veettil MV, Bottero V, Chandran B. 2012. Kaposi's sarcoma-associated
628 herpesvirus interacts with EphrinA2 receptor to amplify signaling essential for productive
629 infection. Proc Natl Acad Sci U S A 109:E1163-1172.
630 35. Dutta D, Chakraborty S, Bandyopadhyay C, Valiya Veettil M, Ansari MA, Singh VV, Chandran B.
631 2013. EphrinA2 regulates clathrin mediated KSHV endocytosis in fibroblast cells by coordinating
632 integrin-associated signaling and c-Cbl directed polyubiquitination. PLoS Pathog 9:e1003510.
633 36. Bandyopadhyay C, Valiya-Veettil M, Dutta D, Chakraborty S, Chandran B. 2014. CIB1 synergizes
634 with EphrinA2 to regulate Kaposi's sarcoma-associated herpesvirus macropinocytic entry in
635 human microvascular dermal endothelial cells. PLoS Pathog 10:e1003941.
636 37. Hahn AS, Desrosiers RC. 2014. Binding of the Kaposi's sarcoma-associated herpesvirus to the
637 ephrin binding surface of the EphA2 receptor and its inhibition by a small molecule. J Virol
638 88:8724-8734.

639 38. Stürzl M, Gaus D, Dirks WG, Ganem D, Jochmann R, G S. 2013. Kaposi's sarcoma-derived cell line
640 SLK is not of endothelial origin, but is a contaminant from a known renal carcinoma cell line. Int J
641 Cancer 132:1954–1958.
642 40. Jarousse N, Chandran B, Coscoy L. 2008. Lack of heparan sulfate expression in B-cell lines:
643 implications for Kaposi's sarcoma-associated herpesvirus and murine gammaherpesvirus 68
644 infections. J Virol 82:12591-12597.
645 41. Brulois KF, Chang H, Lee AS, Ensser A, Wong LY, Toth Z, Lee SH, Lee HR, Myoung J, Ganem D, Oh
646 TK, Kim JF, Gao SJ, Jung JU. 2012. Construction and manipulation of a new Kaposi's sarcoma-
647 associated herpesvirus bacterial artificial chromosome clone. J Virol 86:9708-9720.
648 42. Akula SM, Naranatt PP, Walia NS, Wang FZ, Fegley B, Chandran B. 2003. Kaposi's sarcoma-
649 associated herpesvirus (human herpesvirus 8) infection of human fibroblast cells occurs through
650 endocytosis. J Virol 77:7978-7990.
651 43. Kerur N, Veettil MV, Sharma-Walia N, Sadagopan S, Bottero V, Paul AG, Chandran B. 2010.
652 Characterization of entry and infection of monocytic THP-1 cells by Kaposi's sarcoma associated
653 herpesvirus (KSHV): role of heparan sulfate, DC-SIGN, integrins and signaling. Virology 406:103-
654 116.
655 44. Garrigues HJ, Rubinchikova YE, Dipersio CM, Rose TM. 2008. Integrin alphaVbeta3 Binds to the
656 RGD motif of glycoprotein B of Kaposi's sarcoma-associated herpesvirus and functions as an
657 RGD-dependent entry receptor. J Virol 82:1570-1580.
658 45. Veettil MV, Sadagopan S, Sharma-Walia N, Wang FZ, Raghu H, Varga L, Chandran B. 2008.
659 Kaposi's sarcoma-associated herpesvirus forms a multimolecular complex of integrins
660 (alphaVbeta5, alphaVbeta3, and alpha3beta1) and CD98-xCT during infection of human dermal
661 microvascular endothelial cells, and CD98-xCT is essential for the postentry stage of infection. J
662 Virol 82:12126-12144.

663 46. Garrigues HJ, DeMaster LK, Rubinchikova YE, Rose TM. 2014. KSHV attachment and entry are
664 dependent on αVβ3 integrin localized to specific cell surface microdomains and do not correlate
665 with the presence of heparan sulfate. Virology 464-465:118-133.
666 47. Walker LR, Hussein HA, Akula SM. 2014. Disintegrin-like domain of glycoprotein B regulates
667 Kaposi's sarcoma-associated herpesvirus infection of cells. J Gen Virol 95:1770-1782.
668 48. Myoung J, Ganem D. 2011. Generation of a doxycycline-inducible KSHV producer cell line of
669 endothelial origin: maintenance of tight latency with efficient reactivation upon induction. J
670 Virol Methods 174:12-21.
671 49. Hahn AS, Kaufmann JK, Wies E, Naschberger E, Panteleev-Ivlev J, Schmidt K, Holzer A, Schmidt
672 M, Chen J, König S, Ensser A, Myoung J, Brockmeyer NH, Stürzl M, Fleckenstein B, Neipel F. 2012.
673 The Ephrin Receptor Tyrosine Kinase A2 is a Cellular Receptor for Kaposi's Sarcoma-Associated
674 Herpesvirus. Nat Med 18:961-966.
675 50. Hahn AS, Desrosiers RC. 2013. Rhesus Monkey Rhadinovirus Uses Eph Family Receptors for Entry
676 into B Cells and Endothelial Cells but Not Fibroblasts. PLoS Pathog 9:e1003360.
677 51. Bandyopadhyay C, Veettil MV, Dutta S, Chandran B. 2014. p130Cas scaffolds the signalosome to
678 direct adaptor-effector cross talk during Kaposi's sarcoma-associated herpesvirus trafficking in
679 human microvascular dermal endothelial cells. J Virol 88:13858-13878.
680 52. Wang X, Zou Z, Deng Z, Liang D, Zhou X, Sun R, Lan K. 2017. Male hormones activate EphA2 to
681 facilitate Kaposi's sarcoma-associated herpesvirus infection: Implications for gender disparity in
682 Kaposi's sarcoma. PLoS Pathog 13:e1006580.
683 53. Pitulescu ME, Adams RH. 2010. Eph/ephrin molecules—a hub for signaling and endocytosis.
684 Genes Dev 24:2480-2492.
685 54. Bocharov EV, Mayzel ML, Volynsky PE, Goncharuk MV, Ermolyuk YS, Schulga AA, Artemenko EO,
686 Efremov RG, Arseniev AS. 2008. Spatial structure and pH-dependent conformational diversity of

687 dimeric transmembrane domain of the receptor tyrosine kinase EphA1. J Biol Chem 283:29385-
688 29395.
689 55. Inoue N, Winter J, Lal RB, Offermann MK, Koyano S. 2003. Characterization of entry mechanisms
690 of human herpesvirus 8 by using an Rta-dependent reporter cell line. J Virol 77:8147-8152.
691 56. Kaleeba JA, Berger EA. 2006. Broad target cell selectivity of Kaposi's sarcoma-associated
692 herpesvirus glycoprotein-mediated cell fusion and virion entry. Virology 354:7-14.
693 57. Wang FZ, Akula SM, Sharma-Walia N, Zeng L, Chandran B. 2003. Human herpesvirus 8 envelope
694 glycoprotein B mediates cell adhesion via its RGD sequence. J Virol 77:3131-3147.
695 58. Seiradake E, Harlos K, Sutton G, Aricescu AR, Jones EY. 2010. An extracellular steric seeding
696 mechanism for Eph-ephrin signalling platform assembly. Nat Struct Mol Biol 17:398-402.
697 59. Himanen JP, Yermekbayeva L, Janes PW, Walker JR, Xu K, Atapattu L, Rajashankar KR, Mensinga
698 A, Lackmann M, Nikolov DB, Dhe-Paganon S. 2010. Architecture of Eph receptor clusters. Proc
699 Natl Acad Sci U S A 107:10860-10865.
700 60. Seiradake E, Schaupp A, del Toro Ruiz D, Kaufmann R, Mitakidis N, Harlos K, Aricescu AR, Klein R,
701 Jones EY. 2013. Structurally encoded intraclass differences in EphA clusters drive distinct cell
702 responses. Nat Struct Mol Biol 20:958-964.
703 61. Xu K, Tzvetkova-Robev D, Xu Y, Goldgur Y, Chan YP, Himanen JP, Nikolov DB. 2013. Insights into
704 Eph receptor tyrosine kinase activation from crystal structures of the EphA4 ectodomain and its
705 complex with ephrin-A5. Proc Natl Acad Sci U S A 110:14634-14639.
706 62. Wimmer-Kleikamp SH, Janes PW, Squire A, Bastiaens PIH, Lackmann M. 2004. Recruitment of
707 Eph receptors into signaling clusters does not require ephrin contact. J Cell Biol 164:661-666.
708 63. Janes PW, Griesshaber B, Atapattu L, Nievergall E, Hii LL, Mensinga A, Chheang C, Day BW, Boyd
709 AW, Bastiaens PI, Jørgensen C, Pawson T, Lackmann M. 2011. Eph receptor function is
710 modulated by heterooligomerization of A and B type Eph receptors. J Cell Biol 195:1033-1145.

711 64. Holmberg J, Clarke DL, Frisén J. 2000. Regulation of repulsion versus adhesion by different splice
712 forms of an Eph receptor. Nature 408:203-206.
713 65. Greene AC, Lord SJ, Tian A, Rhodes C, Kai H, Groves JT. 2014. Spatial organization of EphA2 at
714 the cell-cell interface modulates trans-endocytosis of ephrinA1. Biophys J 106:2196-2205.
715 66. Schaupp A, Sabet O, Dudanova I, Ponserre M, Bastiaens P, Klein R. 2014. The composition of
716 EphB2 clusters determines the strength in the cellular repulsion response. J Cell Biol 204:409-
717 422.
718 67. Hynes RO. 2002. Integrins: bidirectional, allosteric signaling machines. Cell 110:673-687.
719
720
721
722
723
724
725
726
727
728
729
730
731
732
733
734

735 **FIGURES**

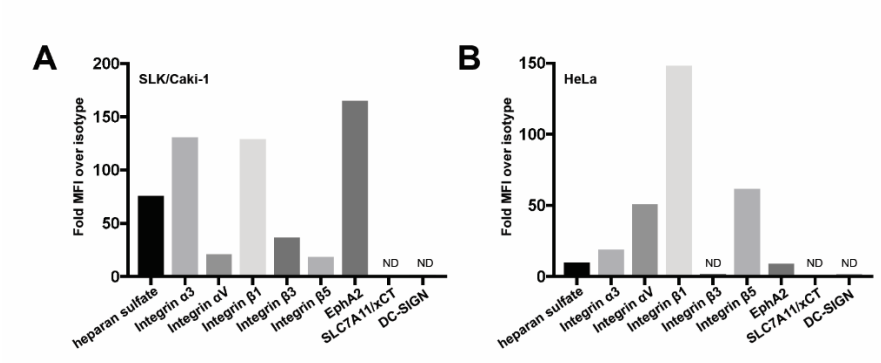

736

737 Figure 1. Surface expression of known KSHV receptors on Caki-1 and HeLa cells.

738

739 Live Caki-1 (A) and HeLa (B) cells were tested for surface expression of known KSHV receptors by

740 immunostaining and flow cytometry. The mean fluorescence intensity (MFI) of each receptor stain was

741 normalized to that of the appropriate primary antibody isotype control. ND, not detected.

742

743

744

745

746

747

748

749

750

751

752

753

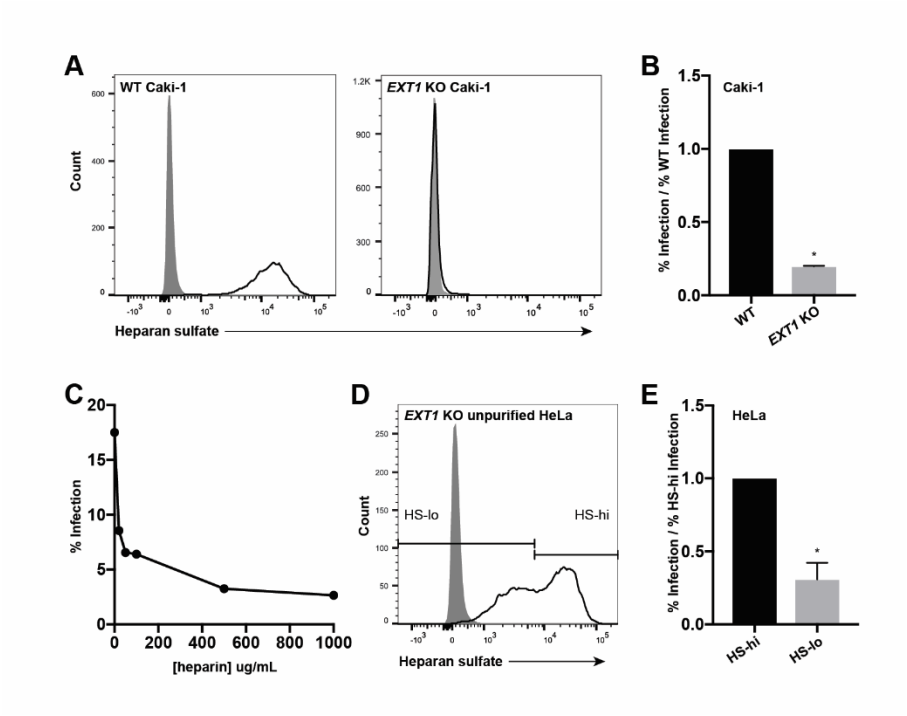

754

755 Figure 2. Heparan sulfate is required for efficient infection of Caki-1 and HeLa cells.

756

757 (A) WT and *EXT1* KO Caki-1 cells were immunostained for surface heparan sulfate (HS) expression. Grey
758 histograms represent isotype controls. (B) WT and *EXT1* KO Caki-1 cells were infected with KSHV in
759 duplicate and infection rates were measured by flow cytometry. The infection rate of the KO was
760 normalized to the average WT infection rate and data was pooled from multiple experiments. (C)
761 Purified KSHV was pre-incubated with the indicated concentrations of soluble heparin which was
762 maintained during infection. Infection rates were measured by flow cytometry. (D) Mixed *EXT1* KO HeLa
763 cells were immunostained for surface HS expression. Grey histogram represents isotype control. (E) The
764 mixed *EXT1* KO HeLa pool was infected with KSHV in triplicate. The pool was immunostained for HS
765 while infection rate was quantified by flow cytometry and cells were gated on HS-high or -low
766 expression as indicated in (D). The infection rate of HS-low cells was normalized to HS-high cells in each
767 well and data was pooled from multiple experiments. *, $p < 0.05$.

768

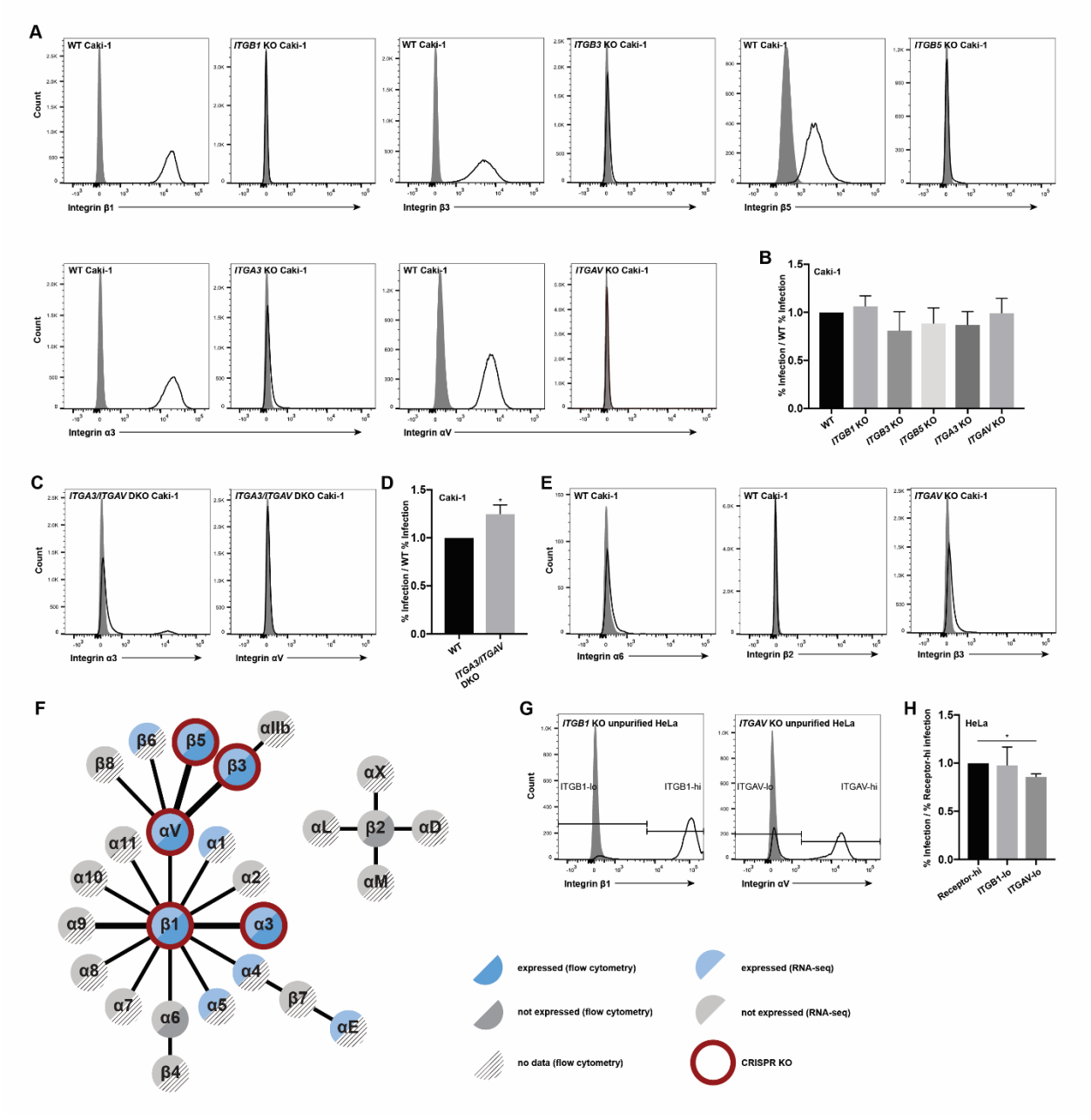

769

770 Figure 3. Integrins are not required for infection of Caki-1 and HeLa cells.

771

772 (A, E) WT and indicated integrin subunit KO Caki-1 cells were immunostained for surface expression of

773 the indicated integrins. Grey histograms represent isotype controls. (B) WT and integrin KO Caki-1 pools

774 were infected with KSHV in duplicate and infection rate was quantified by flow cytometry. The infection

775 rates of the KO pools were normalized to the average WT infection rate and data was pooled from

776 multiple experiments. (C) *ITGA3/ITGAV* double KO Caki-1 cells were immunostained for surface integrin
777 α3 and αV expression. Grey histograms represent the isotype controls. (D) WT and *ITGA3/ITGAV* double
778 KO Caki-1 cells were infected with KSHV in triplicate and infection rate was quantified by flow
779 cytometry. The infection rate of the DKO pool was normalized to the average WT infection rate and data
780 was pooled from multiple experiments. (F) Schematic integrin pairing diagram (adapted from 67)
781 showing expression data measured by surface immunostaining and flow cytometry or RNA-seq analysis.
782 Bold connections denote heterodimers previously implicated in KSHV infection. (G) Mixed *ITGAV* and
783 *ITGB1* KO HeLa cells were immunostained for surface integrin αV and β1 expression. Grey histograms
784 represent the isotype controls. (H) Mixed integrin KO HeLa pools were infected with KSHV in triplicate
785 and infection rates were quantified by flow cytometry. The pools were also immunostained for the
786 corresponding integrins and gated on integrin-high or -low populations as indicated in (G). The infection
787 rates of integrin-low cells were normalized to integrin-high cells in each well and data was pooled from
788 multiple experiments. *, $p < 0.05$.
789
790
791
792
793
794
795
796
797
798
799

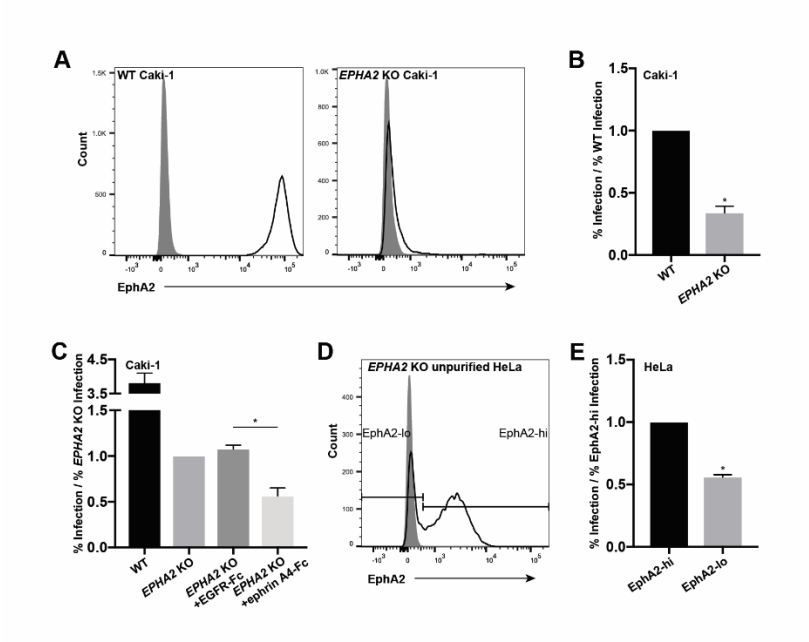

Figure 4. EphA2 is required for efficient infection of Caki-1 and HeLa cells.

(A) WT and *EPHA2* KO Caki-1 cells were immunostained for surface EphA2 expression. Grey histogram represents isotype control. (B) WT and *EPHA2* KO Caki-1 cells were infected with KSHV in duplicate and infection rates were quantified by flow cytometry. The infection rate of the *EPHA2* KO pool was normalized to the average WT infection rate and data was pooled from multiple experiments. (C) *EPHA2* KO Caki-1 cells were pre-blocked with EGFR-Fc, ephrin-A4-Fc, or an equal volume of PBS in media at 10 µg/mL and then infected in triplicate in the presence of EGFR-Fc or ephrin-A4-Fc at 5 µg/mL. Infection rate was measured by flow cytometry and infection rates were normalized to the average *EPHA2* KO infection rate. (D) Mixed *EPHA2* KO HeLa cells were immunostained for surface EphA2 expression. Grey histograms represent the isotype controls. (E) The mixed *EPHA2* KO HeLa cells were infected with KSHV in triplicate and GFP+ cells were quantified by flow cytometry. The cells were also immunostained for EphA2 and gated on EphA2-high or -low as indicated in (D). The infection rates of EphA2-low cells were normalized to EphA2-high cells in each well and data was pooled from multiple experiments. *, $p < 0.05$.

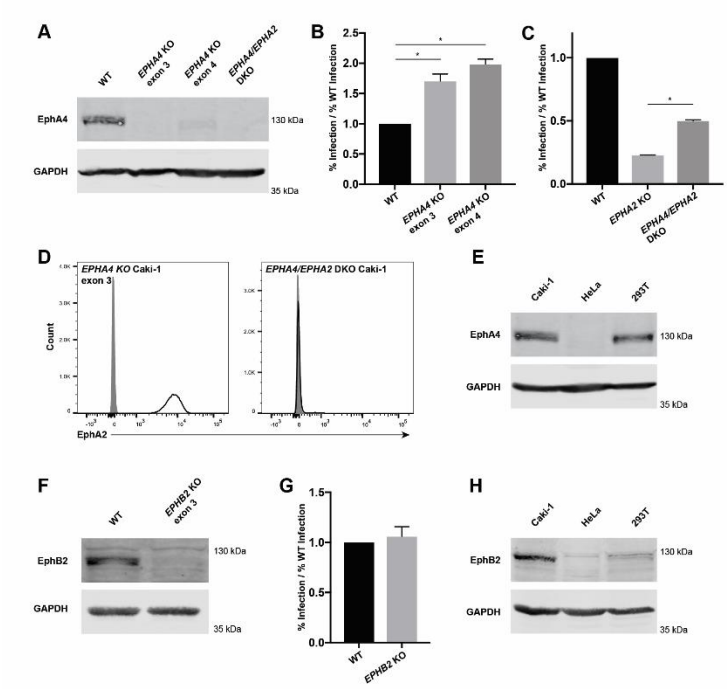

Figure 5. EphA4 and EphB2 are dispensable for infection of Caki-1 cells.

(A, E, H) 120 µg or (F) 50 ug of the indicated cell lysates were run on a 10% SDS-PAGE gel and blotted for EphA4 (A, E) or EphB2 (F, H) and GAPDH as a loading control. WT and *EPHA4* KO Caki-1 cells (B), or WT, *EPHA2* KO, and *EPHA4/EPHA2* DKO Caki-1 cells (C) were infected with KSHV in triplicate and infection rate was quantified by flow cytometry. The infection rates of KO cell lines were normalized to the average infection rate of WT cells and a representative experiment is shown. (D) *EPHA4* KO and *EPHA4/EPHA2* DKO Caki-1 cells were immunostained for surface EphA2 expression. Grey histograms represent isotype controls. (G) WT and *EPHB2* KO Caki-1 cells were infected with KSHV in triplicate and infection rates were quantified by flow cytometry. The infection rates of the KO line were normalized to the average WT infection rate and a representative experiment is shown. *, $p < 0.05$.

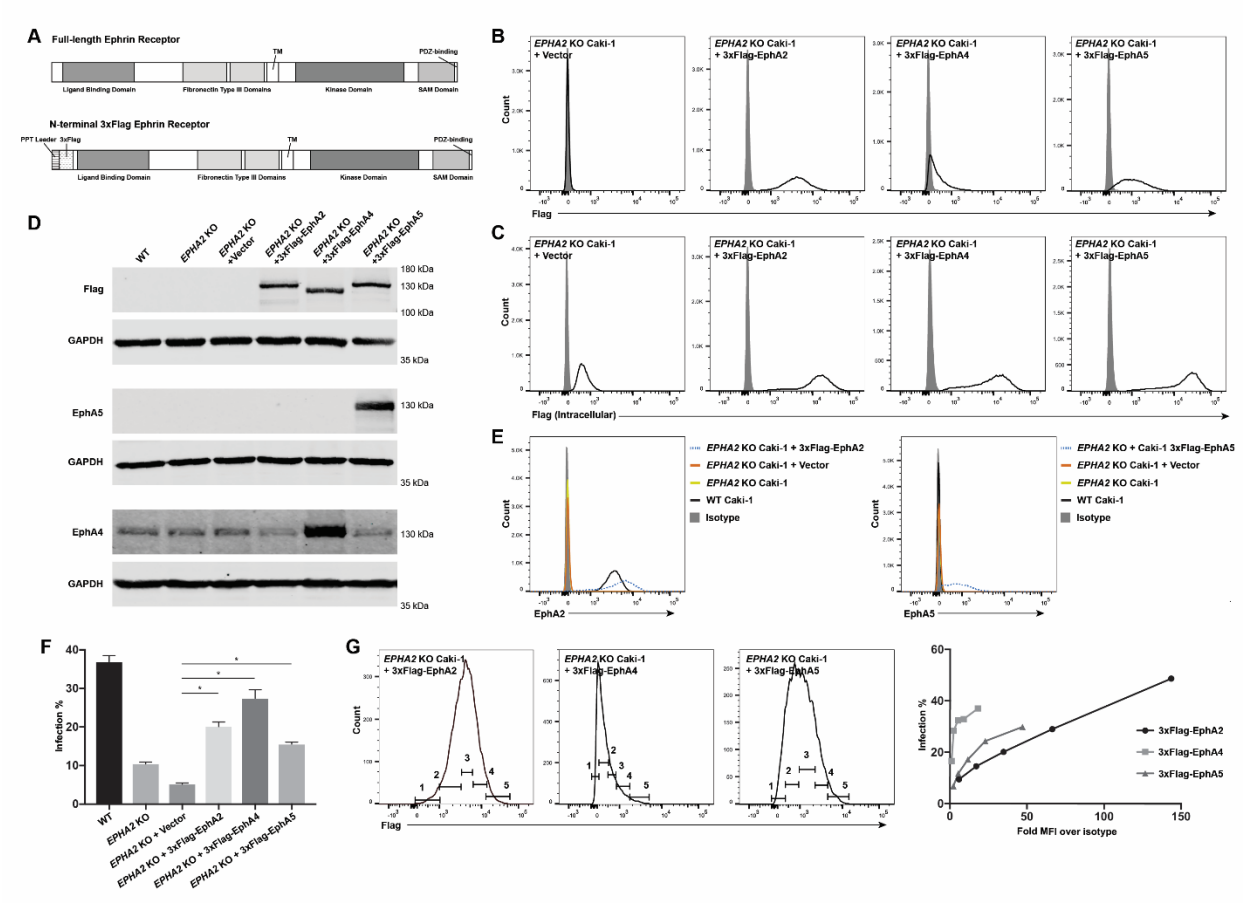

Figure 6. EphA2, EphA4, and EphA5 rescue KSHV infection in *EPHA2* KO Caki-1 cells.

(A) Diagram of generalized full-length and PPT-3xFlag-mature ephrin receptor constructs. Live (B) or fixed and permeabilized (C) 3xFlag-tagged ephrin receptor transduced *EPHA2* KO cells and a vector control were immunostained for surface (B) or intracellular (C) 3xFlag expression and analyzed by flow cytometry. Grey histograms represent isotype controls. (D) The indicated cell lysates were run on 10% SDS-PAGE gels and blotted for 3xFlag, EphA4, and EphA5 with matched GAPDH as a loading control. For the Flag and EphA5 blots, 15 µg of lysate was loaded. For the EphA4 blot, 120 µg of lysate was loaded. (E) The indicated cell lines were immunostained for surface EphA2 or EphA5 expression and analyzed by flow cytometry. Grey histograms represent isotype controls. (F) The indicated cell lines were infected with KSHV in triplicate and infection rate was quantified by flow cytometry. A representative experiment

841 is shown. (G) The 3xFlag expression histograms of infected 3xFlag-tagged ephrin receptor transduced
842 cell lines were divided into five successive gates as shown. The infection rate within each gate was
843 plotted against the fold MFI over isotype of each gate. *, $p < 0.05$.
844
845
846
847
848
849
850
851
852
853
854
855
856
857
858
859
860
861
862
863
864

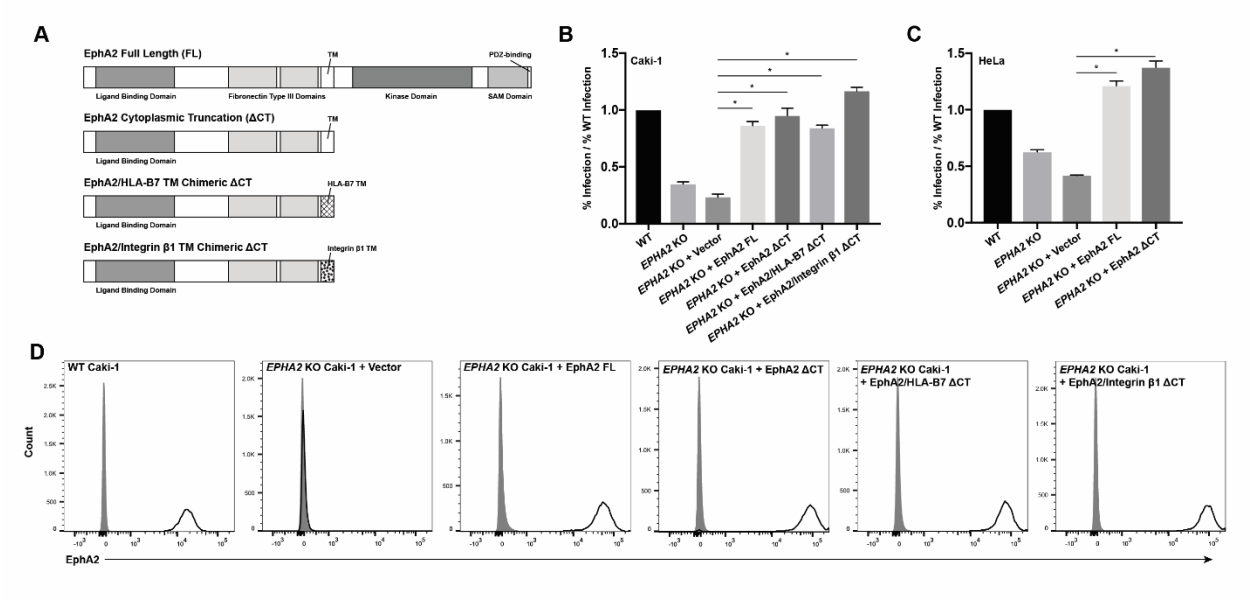

Figure 7. EphA2 ectodomain is sufficient to rescue infection rate in *EPHA2* KO cells.

(A) Diagram of EphA2 truncation and domain swap constructs. (B, C) WT, *EPHA2* KO, and *EPHA2* KO cells transduced with the EphA2 constructs indicated in (A) were infected with KSHV in triplicate and infection rate was quantified by flow cytometry. The infection rates were normalized to the average infection rate of WT cells and a representative experiment is shown. (D) WT, *EPHA2* KO, and the indicated transduced *EPHA2* KO Caki-1 cells were immunostained for surface EphA2 expression and analyzed by flow cytometry. Grey histograms represent the isotype controls. *, $p < 0.05$.

881 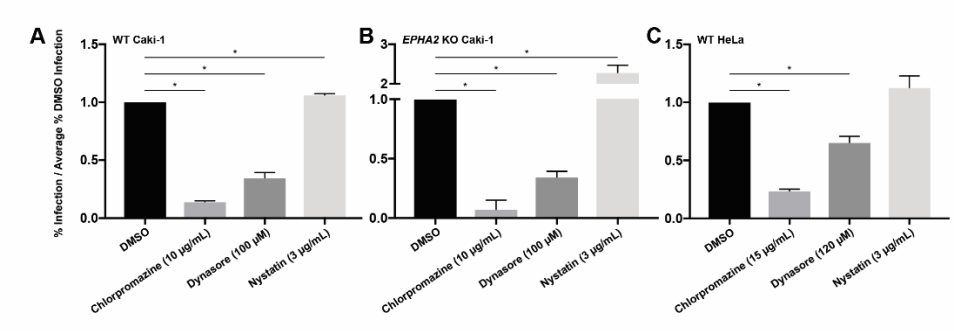

882 Figure 8. KSHV infection of Caki-1 and HeLa cells requires clathrin and dynamin.

883

884 WT Caki-1 (A), *EPHA2* KO Caki-1 (B), and WT HeLa (C) cells were pretreated with the indicated
885 concentrations of chlorpromazine, dynasore, nystatin, or an appropriate volume control of DMSO, then
886 infected with KSHV in triplicate while maintaining the indicated drug concentrations. Infection rate was
887 quantified by flow cytometry. The infection rates of the drug-treated cells were normalized to the
888 average infection rate of the corresponding DMSO-treated cells and a representative experiment is
889 shown for each cell line. *, $p < 0.05$.

890

891

892

893

894

895

896

897

898

899

900

901

902

903 **TABLES**

Gene	Exon	Guide sequence 5'-3'
EXT1	1	GTGGACGAACGACTACTCCA
ITGA3	4	GTCAGAAGACCAGCGGCGCA
ITGAV	2	GTGACTGGTCTTCTACCCGC
ITGB1	3	AATGTAACCAACCGTAGCAA
ITGB3	3	GAGCCGGAGTGCAATCCTCT
ITGB5	1	GCAGGCGTACAGCGGCGCCG
EPHA2	4	GTGTGCAAGGCATCGACGCT
EPHA4	3	TCCACTCACAGTCCGCAATC
	4	TCTGAAAAAGCCTCGGTCAC
EPHB2	3	GAACACGATCCGCACGTACC

904

905 Table 1. CRISPR-Cas9 guide RNA sequences used to target the indicated genes.

906